



Influence of the Sintering Additive (Fe_2O_3) to the Morphological and Microstructural Development of SnO_2 Ceramic Powders

HALIMA CHEMANI^{1,*} and BACHIR CHEMANI²

¹Mineral Materials and Composites Laboratory, University of Boumerdes, Boumerdès 35000, Algérie

²Processing and Formatting of Fibrous Materials and Polymers Laboratory, University of Boumerdes, Boumerdès 35000, Algérie

*Corresponding author: E-mail: chemani_salima@yahoo.fr

(Received: 3 November 2011;

Accepted: 16 June 2012)

AJC-11627

The properties of a large number of materials are conditioned by their microstructure. A simple variation in temperature, the treatment time or the presences of impurities have an influence on them. A systematic study was carried out by adding Fe_2O_3 at content levels of 1 to 2 %, enabling its effect on the micro-structural development of the SnO_2 powder to be observed. The effectiveness of the additive to attain a high density is studied in terms of grain growth. Its surface distribution changes the chemical composition of the latter, decreases the surface energy, increases the specific surface area and diminishes porosity. According to the morphology study carried out by SEM Fractograph and in accordance with the fracture pictures found, it appears that certain pores which stay trapped in the grains do not make the attainment of high densities possible. In present case, iron oxide seems to play quite a low role and belongs to the group D classification, since the sizes of the crystallite calculated by the Debye relation offer values of $D > 18$ nm. To reach densities which are slightly higher, it is necessary to use more rapid thermal treatment.

Key Words: Sintering additive, Fe_2O_3 , SnO_2 , Ceramic powders.

INTRODUCTION

Tin(IV) oxide has been applied for a long time in the chemical reinforcement of spectacles and polycrystalline ceramics in the form of a surface treatment coating¹. Used particularly in the production of bearings and bearing bushes, in the components of machines, filters, diagrams, friction equipment, gas detection and humidity detection². Tin(IV) oxide tends to replace the chromium oxide used in glass refractory, owing to its corrosion resistance capacity. In presence of other ions such as Ca^{2+} , Na^+ and K^+ , chromates are formed, soluble salts in water which are quite harmful. The SnO_2 will be applied as an anti-corrosive layer on the interface between the glass and the traditional refractory (silico-aluminous). The microstructure of a sintered product is determined in accordance with two processes, densification and the growth of particles³. The grain frontier distribution is the main mechanism for densification. When these mechanisms predominate during sintering, high density with small grains is obtained. The relative contribution of the transport mechanisms of the material depends on the sintering conditions and the characteristics of the powder. This sintering phenomena complexity makes the control of microstructure difficult. The sintering of pure SnO_2 arises principally from the evaporation/

condensation mechanism⁴. Shrinkage is low and the size of the grains and pores increases during sintering. Our study clearly points out the work of Quadir and Whittemore⁵. The antagonistic effect of iron oxide on the densification of powders and the other properties depends both on the SnO_2 structure and the interaction of the activity on the grain surface of the latter. It is usually accepted that the Fe^{2+} ion is compensated by the oxygen void in the SnO_2 crystal⁶.

The development of microstructure by adding various Fe_2O_3 contents and various sintering temperatures is studied as a function of the mass transport mechanism. The fracture surfaces of sintered samples are studied using the scanning electron microscope to assess the grain growth and the behaviour of the various densities.

EXPERIMENTAL

Forming pastilles: A series of pastilles were formed using powders which were aged for 1 week, sintered at 700 °C and pressed in dies of 8 mm diameter, with forming under 40 MPa. Two types of analyses were taken into consideration. The first covered the sintering of samples under natural conditions; as for the second type, it was mixed with 1 and 2 % contents of Fe_2O_3 . The thermal treatment was carried out using the three types of temperatures 1000, 1100 and 1200 °C. The sintering

was carried out in a tubular kiln (lifting) model Eurotherm 2408 with maximum temperature of 1200 °C and a sintering cycle of 15 %/min. The main physical parameters examined at the end of the sintering were the volume shrinkage, the linear shrinkage and the density.

The average size of the crystallites was assessed by X-ray diffraction in the hkl planes (110), (101) and (211), registered on a diffract meter based on the Scherrer equation where λ is used with the ray K α 1 of Cu 1554059800. The reflection device is equipped with a 120° curve detector. The crystalline condition examined is determined using direct observation by a Scanning Electron Microscope (Hitachi S2500 with tungsten filament).

For the observation, the sintered samples are reduced into fine granules and then dispersed in acetone under supersonic vibration. A few drops of the diluted suspension are placed on a metal sample carrier and then subjected to morphological observation by imaging.

The study of the fractured surfaces is carried out by SEM using the same apparatus. For this, the pastilles are split into two; the observation is made directly on the fractured part, fixing the pastille half on the sample carrier using silver glue. Determining the average size of the grains is carried out using the linear interception method on the image.

RESULTS AND DISCUSSION

Influence of iron oxide on the behaviour of SnO₂ powder sintering: Sintering of SnO₂ is produced mainly by the evaporation-condensation mechanism. First of all, the SnO₂ microstructure was carried out by considering two physical parameters which are represented in Fig. 1, showing the variation in volume and linear shrinkage depending on the sintering temperature and the content of Fe₂O₃.

Volume shrinkage: The volume shrinkage values of the SnO₂ pure powder samples (without iron oxide) are inversely proportional to the sintering temperatures. This is explained by a sintering stage which has not yet attained its maximum value. The liquid stage is not sufficient to activate the sintering mechanism. Surface tension is still low enough to enable the particles to approach each other. As concerns the final volume value compared to the initial volume, the latter diminishes in accordance with the increase in temperature. This is due to a start of vitrification, which will serve as a cement to connect the particles to each other and providing the best compacting. Volume a shrinkage value of the samples in which iron oxide has been added grows with the increase in the content of the latter. When the sintering temperature increases, the growth is slowed. Samples which contain 2 % have even lower shrinkage. This is probably due to a decrease in the degree of sintering, since this content appears to exceed the critical threshold.

Linear shrinkage: The shrinkage values of the pure SnO₂ powder samples (without iron oxide) are inversely proportional to the sintering temperatures and are rather low. The grains and the pores increase. The pores are open during sintering and non-closed pores are formed. The microstructure becomes homogenous. These characteristics are observed in the system where the predominant sintering mechanism is evaporation-

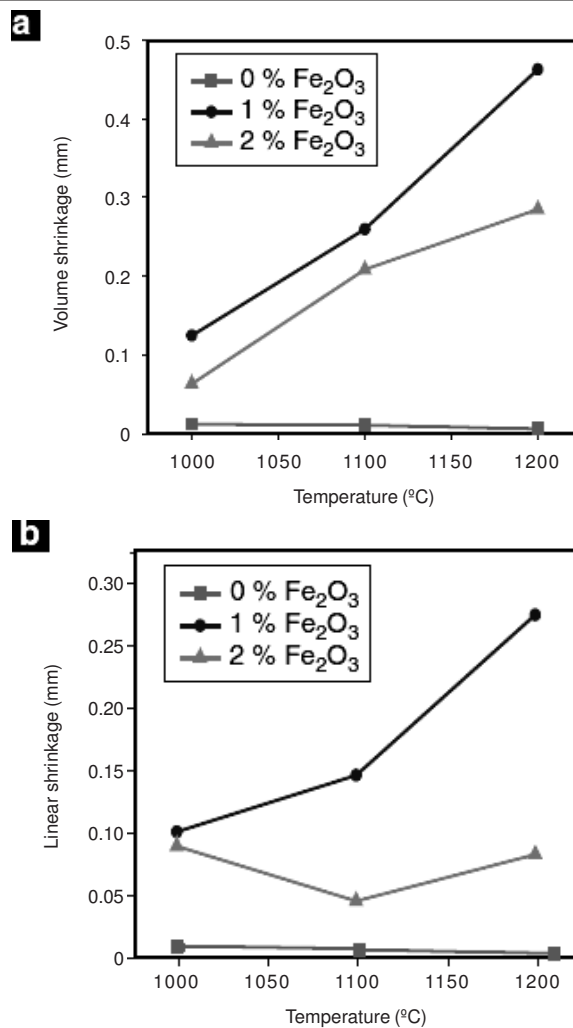


Fig. 1. Influence of the temperature and iron content on: (a) volume shrinkage, (b) linear shrinkage

condensation. As to samples where iron oxide is added, shrinkage increases proportionally with the temperature, due to the partial decomposition of Fe₂O₃ in another form with the formation of another phase. This has indeed been demonstrated by X-ray diffraction analyses⁶.

Apparent densities: The distribution surface for the evaporation-condensation results from the growth of the particles. When only one of these mechanisms is predominant, densification does not take place and high density is hardly attained, since usually densification and grain growth are produced simultaneously⁷.

As indicated in Fig. 2, the density of the sintered products depends on the temperature and on the additive content. Fe₂O₃ supplies an average sintering intensity in the range of 1100-1200 °C. Leading to a low increase in density, it is probable that at high temperatures, the Fe₂O₃ sublimates and reacts with the SnO₂ during the vapour phase. After sublimation, Sn₃O₄ is formed with an increase in concentration defect in the crystal network which encourages sintering. It is usually accepted that the Fe³⁺ are compensated by a void of oxygen in the SnO₂ network⁸. The more iron is added, the more the sintering starts early and ends early, producing powders which are not densified and not too compact. The highest density values are obtained

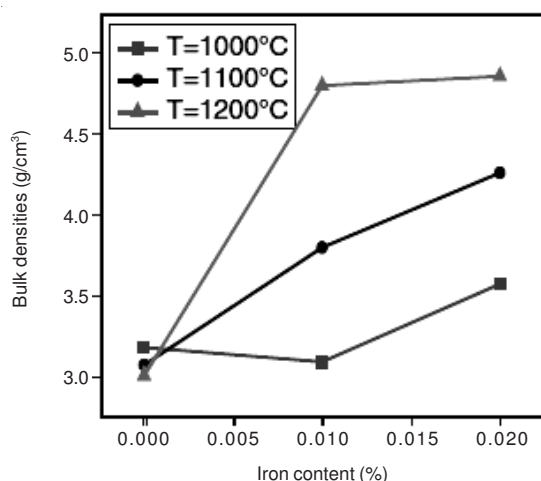


Fig. 2. Variation of density in relation to the temperature and iron content

with an additive content of 2 %, corresponding to a temperature of 1200 °C, which is explained by the complete reduction of Fe^{3+} , which is delayed under the reduced oxygen pressure⁶. For each temperature within the 1000 to 1200 °C range, there is a critical iron oxide content which enables highly densified SnO_2 ceramics to be obtained. The SnO_2 densification in the presence of iron cannot be explained by sintering in the liquid phase, even at temperatures as high as 1200 °C, since under no circumstances are rapid shrinkage values found to be accompanied with high densification. The increase in grain and shrinkage takes place simultaneously. Concerning the powders selected, they seem to be polluted by some impurities which accelerate the growth of the grains and inhibit densification. The products obtained show a value lower than that of the theoretical density (which is of the order of 6.95 g/cm³). This value could only be attained by more rapid heating.

Development of powder morphology during the heat treatment: The products obtained are chemically and morphologically homogenous in the Fe_2O_3 concentration range going from 0 to 2 %. The addition of an appropriate additive content leads to an improvement of the specific surface area and to a growth of the grains. The higher the iron concentration, the larger is the pore surface. The absence of densification during the thermal treatment is explained by a mass transfer controlled by surface distribution at low temperatures and by the condensation-evaporation phenomena at high temperatures.

The results of diffraction phase analysis of samples containing the additive enabled the principal phases to be identified by using the datasheets 21-1250 for the SnO_2 and 00-39-1346, 00-033-0664 for the Fe_2O_3 . In accordance with the diffraction rays, we observe that, regardless of the additive content, the peaks showing the presence of iron are more present at temperatures < 1200 °C, that is to say 1000 and 1100 °C. Their intensities vary greatly and the majority phases are SnO_2 . These iron ions must be located inside the SnO_2 grains or on the surfaces of the grains^{10,11}. It should be noted that the sizes of the peaks for the main rays belong to SnO_2 and since they have a 2 % iron concentration, they diminish with the increase in temperature. Some authors suggest that in samples containing metallic iron, this component disappears after treatment

of the latter in air, following its redispersion in the environment¹². For others, the samples crystallize more and more. For samples with a concentration of 1 %, the width of the peaks decrease at a temperature of 1100 °C and then increase again at 1200 °C, which agrees perfectly with the crystallite size values calculated by the Debye ratio as from the plan (110) (101) and shown on Tables 1 and 2. It is observed that the crystallite sizes are inversely proportional to the width of the peaks. The more the product crystallizes, the more the rays are reduced.

TABLE-1
VARIATION OF THE CRYSTALLITE SIZE IN RELATION TO THE TEMPERATURE AND IRON CONTENT

Properties	1 000	1100	1200
Sintering temperature (°C)	1 000	1100	1200
d110 (nm)	0.335	0.335	0.335
FWhm (rad)	0.00257	0.00203	0.00206
D_{XRD} (nm)	53.84	68.22	67.41
d101 (nm)	0.264	0.264	0.264
FWhm (rad)	0.00270	0.00208	0.00214
D_{XRD} (nm)	51.27	66.69	64.87

Samples containing 1 % of Fe_2O_3 .

TABLE-2
VARIATION OF THE CRYSTALLITE SIZE IN RELATION TO THE TEMPERATURE AND IRON CONTENT

Properties	1 000	1100	1200
Sintering temperature (°C)	1 000	1100	1200
d110 (nm)	0.335	0.335	0.335
FWhm (rad)	0.00255	0.00222	0.00196
D_{XRD} (nm)	54.35	62.47	70.65
d101 (nm)	0.264	0.264	0.264
FWhm (rad)	0.00259	0.00233	0.00208
D_{XRD} (nm)	53.36	59.47	66.55

Samples containing 2 % of Fe_2O_3 .

Role of iron and the stabilization mechanism: SnO_2 is known as a typical oxide conditioned by a sintering method where the increase of the grain takes place with a change in porosity (or apparent density)¹³. Such a method is possible when the grain growth continues *via* a surface diffusion mechanism or the condensation of evaporation¹⁴. In view of the crystallite size values, the iron belongs to group D type (II), this latter seems to have a quite low effect, since $D_{\text{XRD}} > 18$ nm. The additives are considered as effective when they stabilize the SnO_2 crystallites at lower values than 10nm, even after treatment at temperatures >1000 °C. They lose their effects at higher temperatures. As they are subjected to segregation, fusion or sublimation, their disappearance from the SnO_2 crystallite surface seems to be the principal cause of the loss of stabilising effects. At a temperature of 1000 °C, analyses using ray refraction DSEM (μm) confirms the formation of solid solution with SnO_2 as from a few iron ions. When the additive is dispersed and immobilized on the surface of the SnO_2 crystallites, it slows the surface diffusion which leads to a growth in grain of SnO_2 ¹⁵.

Observation of the fracture surfaces using SEM: Characterizing fractures and polished surfaces is not easy when it concerns the ceramics which have low densities and low grain sizes and this is indeed the case of the selected samples.

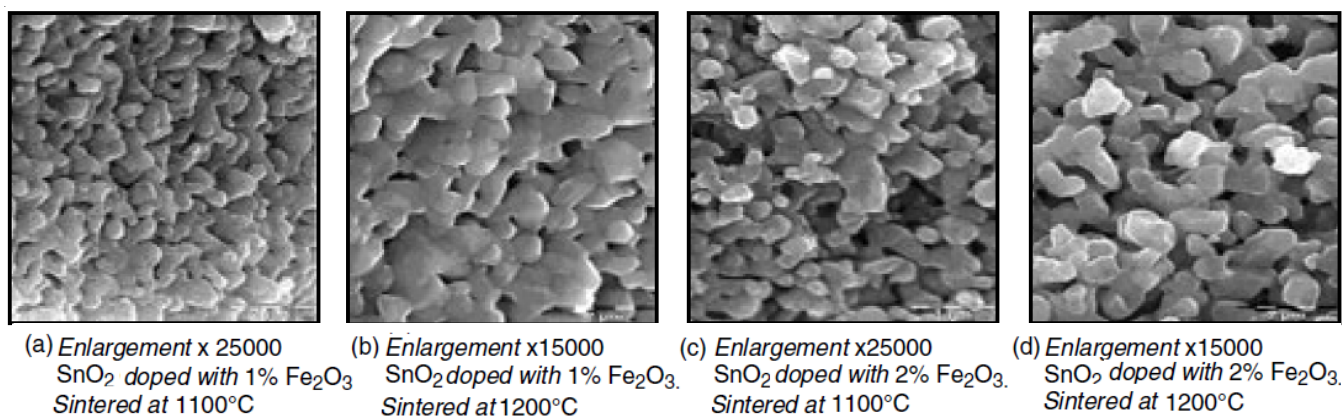


Fig. 3. Images observed on the fractured surface

The thermal treatment and the addition of iron oxide show three phenomena:

- (i) net growth of grains;
- (ii) decrease in pores of about 40% line;
- (iii) crystallization of Fe₂O₃.

which is indeed demonstrated (Fig. 3).

Generally the presence of impurities (sintering additive) modifies the structure surface of a smooth appearance to a rough appearance and has as a result an acceleration of the rate of growth of the ends while the crystal surface remains unchanged. This type of modification can be considered as the kinetic of the surface roughness. By observing the effect of iron on the SnO₂, the fracture surfaces of sintered powders at temperatures of 1000, 1100 and 1200 °C have homogeneous forms with non-roughened grains.

Determining the average size of grains: The average size is determined by and linear interception method on the low grain sizes fractured samples in accordance with the ratio¹⁶:

$$D_{SEM} = 1.65 \frac{L - P}{N}$$

where L = total length; P = lengths of the pores of the sample line traverse; N = intercept number.

The proportionality constant 1.65 is the product of two correction factors: one is due to the shape of the grain (1.50 for spheres)¹⁷ and the second is in relation to the surface roughness (1.1 in accordance with Case *et al.*)¹⁸. The determination of the average size of the grains D_{SEM} of each type of powder is reported in Table-3. Changing the iron content from 0 to 1 % for sintered samples at 1200 °C shows an increase in the average diameter of the grains by more than twice their initial value (0.39 to 0.90 μm). On the other hand, when changing from a content of 1 to 2 %, we observe a slight increase in the grain size for treatment at 1100 and 1200 °C. The ceramics show less pores than those which are treated with 2 % of iron oxide and processed at 1200 °C with an average pore size of 0.93 μm. For each sample, the average grain size is taken as the average value of D_{SEM} determined on each photo of the ceramic. By taking into consideration the measurement errors, the influence of the shape of the grain and the preparation of the sample, it would be possible to estimate the sample to an accuracy of more than 20 %¹⁷. By comparing D_{XRD} calculated

TABLE-3
AVERAGE DIAMETER DETERMINED ON
FRACTURED SURFACES

Properties	0	1	2
Content of sintering additive Fe ₂ O ₃ (%)	0	1	2
Temperature (°C)	1000	1100	1200
D_{SEM} (μm)	0.17	0.20	0.36
	0.21	0.40	0.45
	0.39	0.90	0.93

using the Scherer ratio and D_{SEM} calculated using the linear interception method, we find that these two values are quite different, which is due to the anisotropic character of the grains.

Conclusion

The effect of the addition of iron oxide on the stabilization of SnO₂ particles during sintering was quite low in view of the crystallite size values D_{XRD} which are > 0.18 nm. Knowing that the specific surface area is inversely proportional to the size of the crystallites, this enables us to deduce that there has been an increase in surface energy. To attain lower crystallite sizes, it is possible to carry out sintering on already sintered powders at temperatures < 700 °C, since at these temperatures it was found in a preceding study that smaller crystallites and higher specific surface area areas are obtained. The sintering of SnO₂ takes place by the evaporation-condensation accompanied by grain growth.

The various microstructures obtained are homogenous. Low densities which result can be due either to certain pores remain trapped in the SnO₂ grains or to the fact that one of the mechanisms - either the surface diffusion or the evaporation-condensation, has predominated. To reach higher densities, close to that of the theoretical value, more rapid thermal treatment must be carried out.

REFERENCES

1. R.G. Egdell, *Mater. Sci. Monographs*, **81**, 527 (1995).
2. A.E. Riviello Jr, D. Young and F. Sebba, *Powder Technol.*, **78**, 19 (1994).
3. D.L. Johnson, *Mater. Sci.*, **11**, 137 (1978).
4. S.J. Park, K. Hirota and Hamamura, *Ceram. Internat.*, **10**, 116 (1984).
5. T. Quadir and D.W. Read, *Mater. Sci. Res.*, **16**, 159 (1984).
6. T. Kimura, S. Inada and T. Yamaguchi, *J. Mater. Sci.*, **24**, 220 (1989).
7. I.M. Garcia dos Santos, A.G. de Souza, F.R. Sensato, E.R. Leite, E. Longo and J.A. Varela, *J. Eur. Ceram. Soc.*, **22**, 1297 (2002).
8. L.T. Grigoryan and D. Gedakyan, *Inorg. Mater.*, **12**, 313 (1976).

9. M. Noguez and P. Poix, *Ann. Chim.*, **3**, 335 (1968).
10. J. Cassedanne, *Ann. Acad. Bras. Cien.*, **38**, 265 (1966).
11. V.G. Bhide and S.K. Date, *J. Inorg. Nucl. Chem.*, **31**, 2397 (1969).
12. S. Music, S. Popovic, M. Metikos Hukovic and V. Gvozdic, *J. Mater. Sci. Lett.*, **10**, 197 (1991)
13. K. Ihokura, *Denki Kagaku*, **50**, 99 (1982).
14. S.A. Selim and F.I. Zeidan, *J. Appl. Chem. Biotechnol.*, **26**, 23 (1976).
15. C. Xu, J. Tamaki and N. Yamazoe, *J. Mater. Sci.*, **27**, 963 (1992).
16. J.-C. Wurst and J.A. Nelson, *J. Am. Ceram. Soc.*, **55**, 109 (1972).
17. E.D. Case, J.R. Smith and V. Monthei, *J. Am. Ceram. Soc.*, **2**, C24 (1981).
18. L.J.M.G. Dortmans, R. Morrell and G. de With, *J. Eur. Ceram. Soc.*, **12**, 205 (1993).